Check for updates

AGU ADVANCING EARTH AND SPACE SCIENCE

Water Resources Research

RESEARCH ARTICLE
10.1029/2022WR031964

Transient Retention of Floating Particles Captured by Emergent Vegetation Through Capillarity

Wei Shi[1], Paolo Peruzzo[1], and Andrea Defina[1]

[1]Department of Civil, Environmental and Architectural Engineering, University of Padova, Padova, Italy

Wei Shi and Paolo Peruzzo contributed equally to this work.

Key Points:

- The probability that floating particles are captured by emerging stems is weakly dependent on stem density
- Temporary captures increase with stem density at the expense of permanent captures due to the turbulence generated by vegetation
- Mean retention time of captured particles is inversely related to the mean flow velocity within the canopy

Correspondence to:

P. Peruzzo,
paolo.peruzzo@dicea.unipd.it

Citation:

Shi, W., Peruzzo, P., & Defina, A. (2022). Transient retention of floating particles captured by emergent vegetation through capillarity. *Water Resources Research*, *58*, e2022WR031964. https://doi.org/10.1029/2022WR031964

Received 10 JAN 2022
Accepted 25 MAY 2022

Author Contributions:

Conceptualization: Paolo Peruzzo, Andrea Defina
Data curation: Wei Shi, Paolo Peruzzo, Andrea Defina
Investigation: Wei Shi
Methodology: Paolo Peruzzo
Supervision: Andrea Defina
Writing – original draft: Wei Shi
Writing – review & editing: Paolo Peruzzo, Andrea Defina

Abstract This work presents and discusses a series of experiments focusing on the transport of floating particles, mimicking seeds and propagules, within an array of randomly arranged cylinders mimicking emergent vegetation stems. The focus is on the temporary capture process by which particles colliding with a cylinder are trapped by surface tension for finite but relatively long retention times, thus promoting a large mechanical dispersion. Video analysis of the particle paths within the array shows that the probability of particles being captured, either temporarily or permanently, as well as the mean retention time, vary with flow velocity while being weakly affected by stem density. On the contrary, stem density plays a significant role in determining the frequency of the temporary captures; in particular, the probability of having temporary, rather than permanent, captures increases with vegetation density. We also propose some relationships to predict the probability of having temporary capture events and their mean duration based on experimental results.

1. Introduction

The transport of seeds and propagules by water is a key process for the maintenance, restoration, and colonization of vegetation in wetlands, with positive benefits for the ecology of these areas (De Ryck et al., 2012; Lipoma et al., 2019; Nilsson et al., 2010; Peterson & Bell, 2012). The literature commonly refers to this phenomenon as hydrochory; however, this definition is rather generic and includes different transport and dispersion mechanisms and processes. First, it is important to distinguish whether seeds are buoyant or not; in fact, nonbuoyant seeds behave like suspended sediments and are driven mainly by the hydrodynamic drag force (Chang et al., 2008; Van der Stocken et al., 2015), whereas buoyant seeds move at the free surface and hence are also subject to surface tension and drag due to wind; for this reason, the processes promoting the dispersion of floating seeds turn out more problematic to model.

Problem complexity increases dramatically when seeds possibly interact with emergent vegetation. In this case, a series of interaction mechanisms between floating particles and emerging stems can occur that differently affect and control the transport of seeds. Stems can directly intercept particles by inertia, that is, by the mechanism of inertial impaction (Palmer et al., 2004; Rubenstein & Koehl, 1977), or they can entrain particles into the wake region forming on their backside, that is, through the wake trapping mechanism (Espinosa-Gayosso et al., 2013, 2015). In hydrochory, these occurrences usually determine relatively short delays (Defina & Peruzzo, 2010, 2012) which are nevertheless responsible for a nonnegligible longitudinal dispersion of the particles traveling within the canopy (Liu et al., 2020; Nepf, 1999; Nepf et al., 1997). Stronger and typically longer lasting interactions are due to the net-trapping mechanism, which occurs when a few leaves/stems of one or two adjacent plants weave each other to form a net-like structure that intercepts the floating particle (Defina & Peruzzo, 2010), or due to the capillary force, that promotes collision of buoyant particles against a stem and their capture (Chambert & James, 2009; Defina & Peruzzo, 2010). The latter mechanism, referred to as the Cheerios effect, is caused by an unbalanced distribution of pressure produced by surface tension, σ, that makes two floating bodies attracting each other when they are close enough to cause an asymmetrical rise of the menisci (Peruzzo et al., 2013; Vella & Mahadevan, 2005). The efficacy of this mechanism is positive linked to σ. For instance, the increase of the temperature or the presence of dissolved surfactant in water causes a lowering of σ and hence a reduction of the cheerios effect; however, most applications assume clean water at 20 °C, so that the surface tension is constant and equal to $\sigma = 0.073$ N/m.

While particles experiencing net-trapping are typically captured permanently by vegetation, the fate of a particle interacting with a stem by the Cheerios effect is uncertain (Defina & Peruzzo, 2012). The capability of a stem to permanently capture a particle by capillarity decreases with the increase of flow velocity. When the flow

10.1029/2022WR031964

velocity, U, is lower than a reference velocity, U_e, named escape velocity, the probability that a particle remains indefinitely attached to the stem is close to one. When U exceeds this threshold, the probability that a particle remains stuck to the stem gradually reduces with U increasing and becomes negligibly small for 2 to 3 U_e (Peruzzo et al., 2012, 2016). Experimental investigations by Peruzzo et al. (2012) and Peruzzo et al. (2016) showed that the escape velocity depends on the characteristics of both particle and stem, namely, size, material, and buoyancy; accordingly, U_e embodies all the parameters influencing the capillary attraction mechanism.

Vegetation density, n, here defined as the number of vegetation stems per unit area (m^{-2}), also plays an important role in the dynamics of capture and dispersion of particles (Rudi et al., 2021). In fact, the interaction events between flowing seeds and vegetation occur more frequently with n increasing thus enhancing mechanical dispersion (Chambert & James, 2009; Nepf, 1999; Van der Stocken et al., 2015).

The dependency on n of the efficacy of the capillary attraction is even more intriguing. Experiments to quantify the capture efficiency carried out using one single cylindrical collector, mimicking a stem (i.e., n close to zero), showed that particles hitting the cylinder either are trapped or flow downstream after rolling/sliding along the cylinder surface (Peruzzo et al., 2016). It is important to stress that, when trapped, particles remained indefinitely stuck to the collector. On the contrary, the experiments carried out to study the transport of floating particles within the emergent canopy of flexible plants (Defina & Peruzzo, 2012) and rigid dowels (Peruzzo et al., 2012), in which the stem density was in the range $n = 299$–$1{,}780\ m^2$(Peruzzo et al., 2012), showed that a fraction of the particles captured by capillarity escape and flow away after a random period of time. The average retentions of the particles that experienced these events of temporary capture are of the order of 100 s, that is, much longer than that due to inertial impaction and wake trapping (of the order of 1 s). This long retention time causes a dramatical increase of the mechanical dispersion and a significant reduction of the mean transport velocity of the particles (Shi et al., 2021).

The reason for this different behavior observed in the experiments, that is, nearly no temporary capture events in the experiments with one single cylinder and a significant number of long temporary capture events in the experiments with an array of collectors, is still unknown yet. We speculate that the different behavior could be attributable to neighboring stems (and hence to the stem density) that enhance flow turbulence and generate secondary wake regions (White & Nepf, 2003) so that captured particles are exposed to highly random velocities that can drag them downstream away from the cylinder. The present work aims to investigate this latter issue through flume experiments, that is, to verify if stem density is the actual reason for the observed different behavior and, if this is the case, to quantitatively relate stem density to (a) the probability of occurrence of long temporary captures and (b) the mean retention time.

2. Materials and Methods

2.1. The Stochastic Model

The purpose of the present investigation is to gain further insight into some aspects of the propagation of floating particles in the presence of emergent vegetation through laboratory experiments. In particular, the temporary capture process when floating particles are captured by capillarity is explored.

Before describing the experiments performed, it is worth shortly recalling the structure and the parameters of the stochastic Lagrangian model proposed by Defina and Peruzzo (2010). Figure 1 shortly illustrates the random walk of a floating particle within a region of emergent vegetation. Along its generic trajectory, a particle encounters a stem, on average, every $\Delta s = {}^{1}\!/\!\sqrt{n}$, where Δs is the mean center-to-center distance between adjacent stems. Within each segment Δs, a particle has the probability P_i of interacting with the stem and the probability $1 - P_i$ of flowing downstream undisturbed.

If a particle interacts with a stem, it can be retained either temporarily, with probability P_t, or permanently, with probability P_c, or it can slow down with probability $1 - P_t - P_c$. The overall probability that a particle is captured by a stem, either temporarily or permanently, is defined as $P_c + P_t$. When a particle is temporarily trapped, it remains attached to the stem for a random time, exponentially distributed with mean value, T.

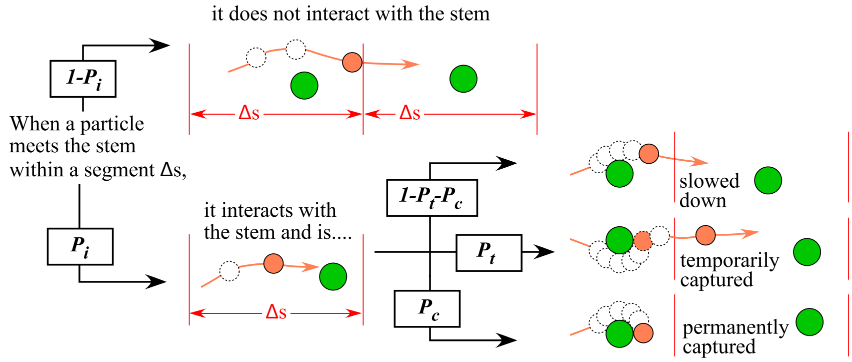

Figure 1. Layout of the stochastic model, adapted from Defina and Peruzzo (2010).

2.2. The Evaluation of Model Parameters

Shimeta and Jumars (1991) and Palmer et al. (2004) proposed a capture efficiency, η, defined as the ratio between b, the spanwise distance between the outmost trajectories leading to collision, and d, the diameter of the stem, that is, $\eta = b/d$, to describe the probability of interaction between floating particles and the stem. Peruzzo et al. (2012) further provided a theoretical formulation to estimate the efficiency, finding that, for given particle and cylinder materials and size, η is inversely proportional to the square root of the ratio U/U_e. Liu et al. (2018) proposed a new definition of the probability of interaction, taking the effect of stem density into consideration, as the ratio between b and the center-to-center distance between adjacent stems, Δs.

In this research, the effect of stem density on the probability of interaction P_i is also investigated as $P_i = b/\Delta s = \sqrt[b]{n}$ (Defina & Peruzzo, 2012). Based on the link between b and η, the probability of interaction between floating particles and the stem P_i can be written as

$$P_i = \frac{b}{\Delta s} = \eta\sqrt{nd} \tag{1}$$

According to the inversely proportional relationship between η and the square root of the ratio U/U_e, the probability of interaction P_i is thus proportional to the square root of $nd^2(U_e/U)$.

When a particle collides with a stem, it is permanently captured if the capillary force is greater than the drag exerted on the particle. In the case of a single emergent cylinder, the local velocity field around the stem is relatively smooth, and thus the fate of the particle mainly depends only on the colliding position around the cylinder. Peruzzo et al. (2016) suggested a semiempirical model to predict the probability of capture by one single emergent cylindrical collector, that is, when $n \to 0$. We define this probability as P_{c0}, and according to the proposed stochastic approach, it reads

$$P_{c0} = \int_0^{U_e/U} f(x)dx \qquad \text{with} \qquad f(x) = \frac{x^{\alpha-1}e^{-x/\beta}}{\beta^{\alpha}\Gamma(\alpha)} \tag{2}$$

In the above equations, $f(x; \alpha, \beta)$ is the gamma distribution with $\Gamma()$ the gamma function, and α and β, respectively, the shape and rate parameters of the gamma distribution. The latter are related to each other as

$$0.95 = \int_0^1 f(x)dx \tag{3}$$

In contrast, hydrodynamics is rather complex within an array of cylinders, and the local velocity around the collector displays a large variability in time. In this case, the local drag force may randomly overcome the capillary attraction and detach previously captured particles, leading to temporary capture events. We speculate that the temporary captures are a fraction of the permanent captures observed with a single collector, that is, in an array the probability of capture $P_c + P_t$ is negligibly affected by stem density, and it can be predicted according to

$$P_c + P_t \approx P_{c0} = \int_0^{U_e/U} f(x)dx \tag{4}$$

10.1029/2022WR031964

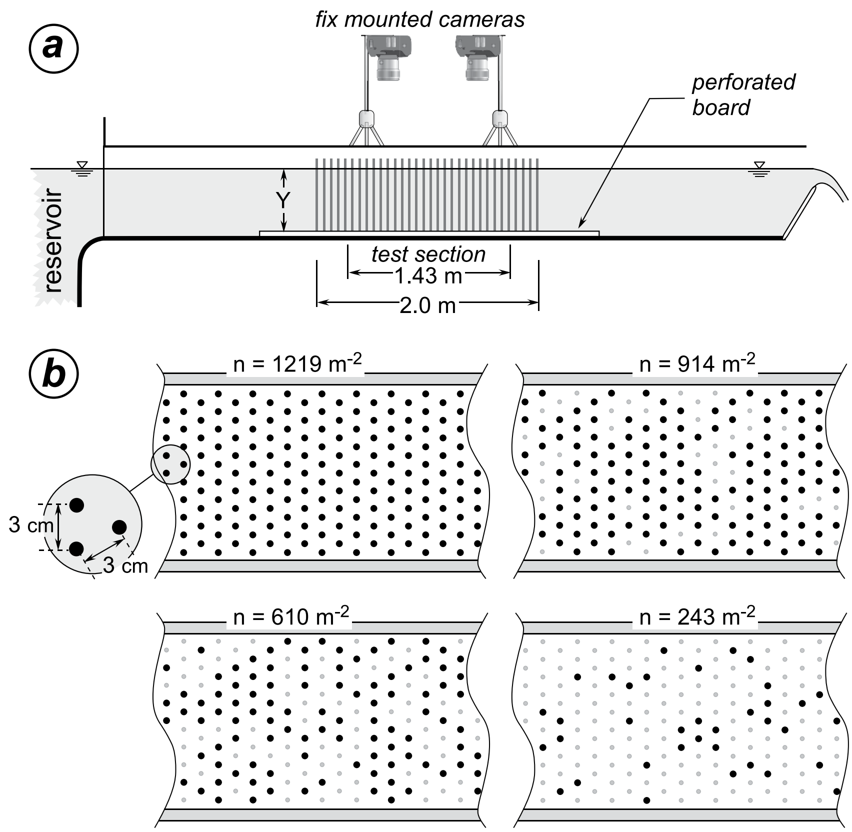

Figure 2. The experimental apparatus: (a) Sketch of the test section with the array of cylinders within the artificial flume and the two fixed mounted cameras; the flow is from left to right. (b) Schemes of the cylinders' disposition for the four densities, *n*, tested.

Therefore, the probability of capture $P_c + P_t$ depends on two parameters, that is, U/U_e and either α or β, or a combination of the two.

2.3. The Experiments

The experiments are carried out in a 6 m long, 0.3 m wide tilting flume where an array of rigid wooden cylinders with a diameter d = 5.5 mm is placed on a perforated Plexiglas board to create a test section of length L = 1.43 m. Water is recirculated through a constant head tank that maintains steady flow conditions. Uniform flow is achieved in the test section by adjusting the bed slope and a downstream weir and by ensuring that the differences between the depths of the water just upstream and downstream of the test section are smaller than 1 mm; uniform flow depth, Y, is chosen in the range between 10 and 15 cm to prevent the formation of transverse seiches induced by the vortex shedding behind the cylinders (Defina & Pradella, 2014; Viero et al., 2017). However, the water is shallow enough to keep the collectors emerging on the free surface. Small wooden spheres of diameter d_p = 6 mm and relative density of 0.65 are released just upstream of the test section and their trajectories are recorded with two fixed mounted cameras with a frame rate of 25 s^{-1} (Figure 2), until the particle either flowed out of the survey area or remained trapped for more than an observation time, t_{obs}, that was fixed equal to t_{obs} = 600 s. The particles are evenly painted blue to improve their observation and tracking. Recorded frames are then extracted and used to accurately determine the characteristics of each particle trajectory, that is, the number and type of interaction events, the particle velocity, and the time that the particles spent attached to a stem when temporarily captured.

Three sets of experiments are carried out. The first series of experiments, labeled A, is designed to investigate the impact of the stem density, n, on the mechanisms of interaction and retention. U is almost equal in all the experiments ($U \approx 5.5$ cm/s), while n varies from 243 to 1,219 m^{-2}. In the test with the maximum density $n = 1,219$ m^{-2},

Table 1
Summary of Experimental Data

Experiments set	Exp.	n (1/m^2)	U (m/s)	T_{obs} (s)	N_0	N_i	N_t	N_c
A	A1	1,219	0.057	237	7,235	2,130	94	113
	A2	914	0.057	239	8,171	1,977	47	150
	A3	610	0.054	250	5,013	1,114	14	202
	A4	243	0.055	249	4,234	689	8	187
B	B1	1,219	0.067	137	15,257	3,282	243	49
	B2	1,219	0.061	139	13,568	2,989	237	97
	B3	1,219	0.058	198	7,654	1,757	172	161
	B4	1,219	0.045	249	1,178	350	20	307
	B5	1,219	0.055	245	4,930	1,368	83	123
	B6	1,219	0.061	207	4,431	1,119	86	48
	B7	1,219	0.062	177	8,268	2,159	146	58
C	C1	610	0.047	194	2,322	453	12	331
	C2	610	0.054	250	3,967	827	31	289
	C3	610	0.058	240	5,256	1,011	34	228
P	P1	1,780	0.029	43				
	P2	1,780	0.035	49				
	P3	1,780	0.041	46				
	P4	1,780	0.047	40				

Note. Experiments denoted with labels P1–P4 are from Peruzzo et al. (2012); n is the stem density, U is the surface velocity, T_{obs} is the average time spent by particles attached to a stem for temporary capture events that last less than t_{obs}, N_0 is the number of segments traversed by particles, N_i is the number of particle-cylinder interactions, N_t is the number of observed long-time retention events shorter than t_{obs}, and N_c is the number of observed events with retention time $\tau > t_{obs}$ regardless of whether the particle is temporarily or permanently trapped.

a staggered arrangement of cylinders is adopted, whereas in the other tests, the cylinders are randomly arranged (see Figure 2b). It is worth noting that in this range of n, the mean distance between two adjacent cylinders is $\Delta s > 5d$, resulting in an average flow velocity only slightly affected by the distribution of the upstream cylinders (Chang & Constantinescu, 2015). The other two sets of experiments, labeled B and C, explore the impact of flow velocity and are carried out with n constant and equal to 1,219 and 610 m^{-2}, respectively. Finally, with label P, we report some unpublished data from Peruzzo et al. (2012) to further study the role of the flow velocity on the retention process. It is worth noting that the particles in the latter experiments had a diameter of 3 mm and a relative density of 0.7 and therefore were different from the particles used in this research.

2.4. The Procedure to Estimate, T, P_t, and P_c

Since the residence time distribution does not have an upper boundary, to correctly estimate the mean retention time T we should extend observation of temporary capture events for extremely long periods. The same problem affects the estimation of the probabilities P_t and P_c since we need to distinguish very long-time capture events from permanent captures. As an alternative, we can estimate T and P_t by extrapolating the results obtained by observing temporary capture events for moderately long periods. This observation time, t_{obs}, is typically much longer than the mean retention time, T; consequently, the extrapolation is likely fairly reliable.

We consider all temporary capture events that last less than t_{obs}, and compute the average time spent by particles while remaining attached to a stem, T_{obs}. By assuming that the residence time of temporary capture events, τ, is randomly distributed according to an exponential probability density function

$$p(\tau) = \frac{1}{T} e^{-\tau/T} \tag{5}$$

we find

$$T_{obs} = \frac{\int_0^{t_{obs}} \tau p(\tau) d\tau}{\int_0^{t_{obs}} p(\tau) d\tau} = \frac{1 - \left(1 + \frac{t_{obs}}{T}\right) e^{-t_{obs}/T}}{1 - e^{-t_{obs}/T}} T \tag{6}$$

The estimated mean residence time, T, is implicitly given by Equation 6 regardless the duration t_{obs}.

The estimation of the probabilities P_t and P_c is also uncertain if the observation time is relatively short. To improve the accuracy in the estimation of these probabilities, we extrapolate the observed number of captures both shorter and longer than t_{obs}, similarly to what we have done to estimate the mean residence time, T.

Let N_i be the total number of the observed particle-stem interactions, N_t the number of the long-time retention events shorter than t_{obs}, and N_c the number of events with retention time $\tau > t_{obs}$ regardless of whether the particle is temporarily or permanently captured. The ratio N_t/N_i gives the probability that a particle is temporarily trapped for a time shorter than t_{obs}. Therefore, by assuming that the distribution of residence time of temporary capture events is given by Equation 5, we can write

$$\frac{N_t}{N_i} = P_t \left(1 - e^{-t_{obs}/T}\right) \tag{7}$$

and hence

$$P_t = \frac{1}{1 - e^{-t_{obs}/T}} \frac{N_t}{N_i} \tag{8}$$

Table 2
Summary of Present Experimental Results

Exp.	P_i (%)	P_t (%)	P_c (%)	T(s)	$P_c/(P_t + P_c)$	$P_c/(P_t + P_c)$ tuned
A1	29.4	6.0	3.7	461.1	0.38	0.42
A2	24.2	3.3	6.6	480.9	0.67	0.69
A3	22.2	1.9	17.5	583.9	0.90	0.90
A4	16.3	1.7	26.5	576.3	0.94	0.94
B1	21.5	7.5	1.4	147.1	0.15	0.19
B2	22.0	8.1	3.1	150.1	0.28	0.30
B3	22.9	11.0	7.9	273.8	0.42	0.44
B4	43.3	8.6	84.7	573.4	0.91	0.92
B5	27.7	9.0	6.1	534.3	0.40	0.48
B6	25.3	8.9	3.1	302.2	0.26	0.30
B7	26.1	7.2	2.2	218.3	0.24	0.28
C1	19.5	2.8	72.8	261.7	0.96	0.97
C2	20.8	5.9	32.8	594.5	0.85	0.88
C3	19.2	4.7	21.2	484.4	0.82	0.82

Note. P_i is the probability of interaction between floating particles and stem calculated with Equation 1; P_t and P_c are the long-time and permanent capture probabilities computed with Equations 8 and 9, respectively; T is the mean residence time estimated with Equation 6; the last column of the table gives the value of the ratio $P_c/(P_t + P_c)$ obtained from the best fitting of experimental data to Equation 10.

In addition, the probability that a particle remains trapped for a time longer than t_{obs}, regardless of whether the capture is temporary or permanent is N_c/N_i

$$\frac{N_c}{N_i} = P_t e^{-t_{obs}/T} + P_c \tag{9}$$

Once P_t is estimated with Equation 8, P_c can be easily computed with the above Equation 9.

To check the above assumptions and extrapolation procedures through the comparison with experimental data, we suitably combine the permanent and long-time temporary capture events by introducing the probability that a particle remains trapped for a time τ larger than t as

$$P(\tau < t) = \frac{P_t}{P_t + P_c} e^{-t/T} + \frac{P_c}{P_t + P_c} \tag{10}$$

3. Results and Discussion

Results of the video analysis of the computed T_{obs}, N_0, N_i, N_t, and N_c are summarized in Table 1, while the stochastic model parameters P_i, P_t, P_c, and T, are reported in Table 2.

Figure 3 shows the relationship between the probability of interaction, P_i, and the density of the stems, n, and the surface velocity, U. Both the present experimental data, denoted by blue circles, and the results given by the experiments carried out by Peruzzo et al. (2012) (red points) are well interpolated by a straight line, indicating that P_i is proportional to the square root of $nd^2(U_e/U)$. The lines interpolating the two data set have different slopes, since the proportionality of P_i with the square root of $nd^2(U_e/U)$ depends on the particle and cylinder materials and size.

We speculate that the probability that a particle remains attached to a stem after colliding with it, that is, the probability of capture $P_c + P_t$, is negligibly affected by stem density n, while depends on the local flow field around the stem U/U_e, and the parameter α or β. In order to verify this assumption, specific experiments with one single vertical cylinder are then carried out following the same procedure used by Peruzzo et al. (2016). From a best fit of Equation 4 to the experimental data, we find $\alpha = 90$, $\beta = 0.0094$ and $U_e \approx 0.046$ m/s. Interestingly, in these experiments the temporary capture event is never observed.

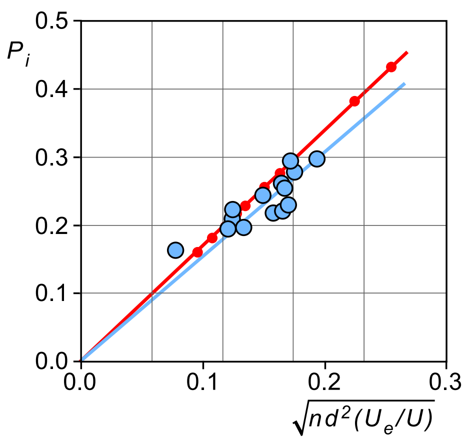

Figure 3. The probability of interaction P_i as a function of $[nd^2(U_e/U)]^{1/2}$. The blue circles denote present experimental data, interpolated by the blue straight line; the red line and points denote the results reported by Peruzzo et al. (2012).

Figure 4 compares the probability of capture P_{c0} as a function of U/U_e estimated in the experiments that use one single cylinder with the distribution of $P_c + P_t$ measured in the experiments with an array of cylinders (Set A). With some approximation, the two series of experimental data agree with each other, thus confirming the validity of the proposed hypothesis.

To compare the probability of exceedance given by Equation 10 with experimental data, we apply the following procedure. For each experimental condition, we sort the $N_t + N_c$ measured retention times in ascending order. The observed probability $P(\tau > t_i)$, with t_i the ith retention time out of the $N_t + N_c$ capture events, and $i = 1, N_t$, is then given by $P(\tau > t_i) = 1 - i/(N_t + N_c)$.

From the comparison between experimental data and Equation 10, we observed that the mean residence time, T, estimated with Equation 6 allows to accurately describe the rate of decay of the probability $P(\tau > t)$. On the contrary, the coefficient $P_t/(P_t + P_c)$ (and hence the coefficient $P_c/(P_t + P_c) = 1 - P_t/(P_t + P_c)$) that uses the probabilities P_t and P_c computed with Equations 8 and 9, respectively, needs to be slightly tuned. Figure 5a

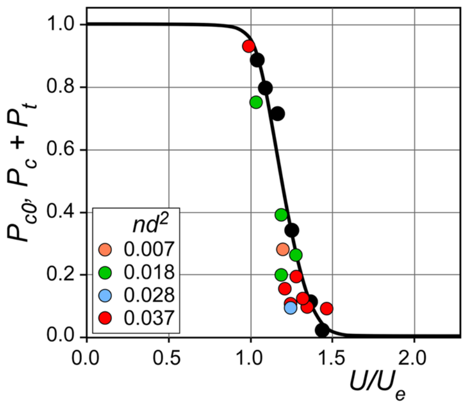

Figure 4. Comparison between the theoretical and experimental probability of capture as a function of U/U_e. The black circles denote the experimental values of P_{c0} measured in the single-cylinder experiments and the black line interpolates these points according to Equation 2; the colored circles denote the measured probability $P_t + P_c$ in the experiments with an array of cylinders.

shows some examples of the comparison between the experimental data and Equation 10 in which the coefficient $P_t/(P_t + P_c)$ is estimated by a best fitting procedure. Importantly, as confirmed by Figure 5b, the adjusted coefficient $P_c/(P_c + P_t)$ turns out to be negligibly larger than the theoretical one computed with the probabilities P_t and P_c given by Equations 8 and 9.

We also observed that the fraction of captured particles that, with equal velocity U (Set A), are permanently captured, $P_c/(P_c + P_t)$, decreases with increasing stem density (see Figure 6). This observation is consistent with the experiments performed using one single cylinder (Peruzzo et al., 2016), in which only a negligibly small number of particles was temporarily trapped.

The reason why temporary capture events increase as n increases, at the expense of permanent captures, is related to the altered hydrodynamics produced by the vegetation. The vegetation enhances the turbulence and the heterogeneity of the velocity field mainly because of the vortexes shed behind each stem and their mutual interaction. Based on this reasoning we expect that the increase of the fraction $P_t/(P_t + P_c)$ with n increasing is related to the turbulence intensity and, in particular, to the turbulent kinetic energy, k, generated by the cylinders. According to the relationship proposed by Nepf (1999) we write

$$k = \alpha_k \left(C_D n d^2\right)^{2/3} U^2 \tag{11}$$

with C_D the bulk drag coefficient and α_k a calibration factor. In the present experiments, conditions are such that $C_D \approx 1$. Accordingly, as a first approximation, we fixed $C_D = 1$ and consider k/α_k as a variable of the problem.

Figure 7 shows the fraction of temporary captures, $P_t/(P_t + P_c)$, as a function of the scaled turbulent kinetic energy $k/(\alpha_k U_e^2)$; the experimental data gather satisfactorily on the black solid line given by the following interpolation equation

$$\frac{P_t}{P_t + P_c} = \frac{1}{1 + \left(0.155/\frac{k}{\alpha_k U_e^2}\right)^4} \tag{12}$$

The suitability of the above relationship between $P_t/(P_t + P_c)$ and $k/(\alpha_k U_e^2)$ is evident also in Figure 6 where Equation 12 is plotted for some values of the velocity U, and compared with the present experimental data.

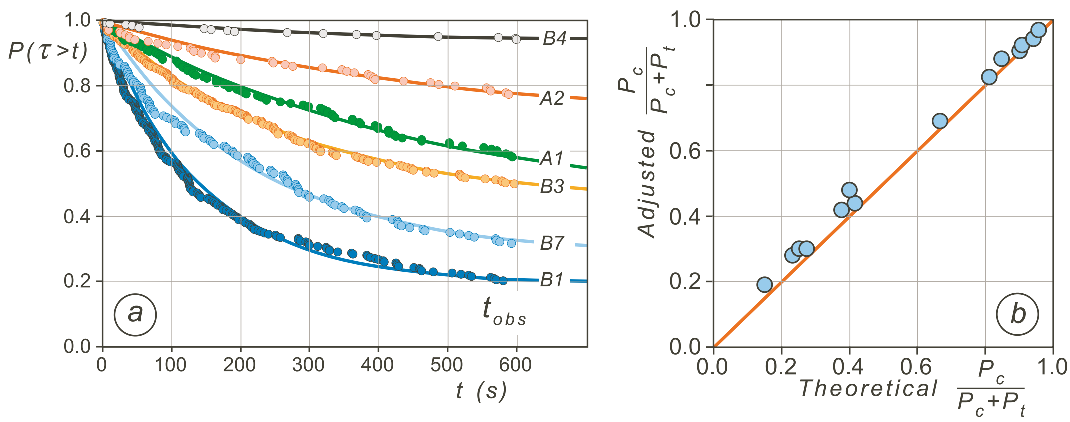

Figure 5. (a) Comparison between experimental and theoretical residence time distribution for six different cases. The circles denote the experimental data and the solid lines are given by Equation 10; the numbers in brackets denote the experiment label. (b) Comparison between adjusted and theoretical $P_c/(P_c + P_t)$.

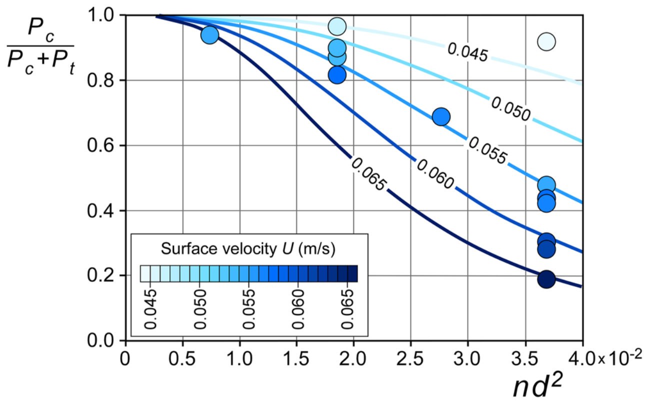

Figure 6. The relative probability of capture $P_c/(P_c + P_t)$ as it varies with the stem density, n; circles are present experimental data, the thick colored lines are from Equation 12 for some values of the surface velocity, U.

Lastly, we estimate the mean residence time, T and its dependence on vegetation, particles and flow characteristics. The time scale of turbulent eddies produced by the cylinders is d/U; interestingly, this time scale is also proportional to the vortex shedding period. Therefore, we use d/U to scale the mean residence time, T. We then observe that TU/d is highly and inversely related to the relative velocity U/U_e and when U/U_e is smaller than one, the probability that a particle is temporarily or permanently captured when it collides with a cylinder is close to one.

When $P_t + P_c \approx 1$, residence times turn out to be extremely long and distinguishing temporary from permanent captures makes no sense; accordingly, we can confidently assume, as an approximation, that $TU/d \to \infty$ when $U/U_e \to 1$ and plot TU/d as a function of $U/U_e - 1$ (Figure 8).

To better assess the relationship between the relative mean residence time TU/d and U/U_e, we also estimate the mean retention time, T, for some of the experiments performed by Peruzzo et al. (2012) (Set P of Table 1). In these experiments, small wooden particles of size 3 mm and 0.7 relative density, labeled as Particle C, were continuously released upstream of an array of maple cylinders of diameter $d = 6$ mm and density $n = 1{,}780$ m^{-2} for about 300 s. The paths of the particles, as well as their interactions with the cylinders, and retention times, were recorded with a fixed mounted camera with a frame rate of 5 s^{-1}. Four series of experiments were carried out by increasing the surface velocity, U, from approximately 2.9 to 4.7 cm/s; the escape velocity was estimated to be $U_e = 1.6$ cm/s, that is, appreciably smaller than that of the present experiments.

To extract reliable statistics, we reanalyze the video-recorded paths after setting the duration of the observation to $t_{obs} = 150$ s; we then measured T_{obs} (see Table 1) and estimated the mean residence time, T, with Equation 6.

Figure 8 also shows that the experimental values of TU/d as a function of U/U_e can be interpolated by the following power law

$$\frac{TU}{d} = \left(\frac{c_1}{U/U_e - 1}\right)^{c_2} \qquad \text{with} \quad c_1 = 140 \text{ and } c_2 = 1.3. \tag{13}$$

The results show satisfactory agreement between the measured and predicted mean retention time through Equation 13 ($R^2 = 0.993$), except for the test $P1$, where the velocity was $U = 2.9$ cm/s. At this low velocity, most of the captures were permanent and the number of temporary captures was relatively small. Consequently, the collected data at this flow velocity probably cannot represent the retention time distribution, resulting in a value of T that deviates from the proposed power law.

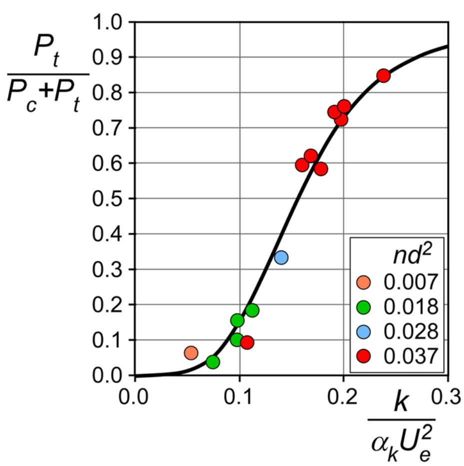

Figure 7. The fraction of particles that are temporarily captured among all the captures, $P_t/(P_c + P_t)$, as a function of the scaled turbulent kinetic energy $k/(\alpha_k U_e^2)$.

Interestingly, the major role that vegetation density plays in the dynamics of floating particles by affecting the temporary capture process, and hence the mechanical diffusion, inspires some considerations about the hydrochory process in areas with emergent vegetation.

Within a newly vegetated area, with sparse vegetation, each stem can trap seeds with a large probability of permanent capture, P_c, thus promoting the local seedling establishment and vegetation thickening. With the increasing of vegetation density, flow velocity reduces, so that the interaction probability (Figure 3) and the probability of capture, $P_c + P_t$ (Figure 4), both increase. At the same time, if the velocity reduction is not excessive, the turbulence, and hence the ratio $P_t/(P_c + P_t)$, also increases (Figure 7) so that a part of the captured seeds are likely captured only temporarily, thus preserving a window of opportunity for seeds to spread longer distances and colonize new areas.

The inherent nonlinearity of the particle-stem interaction process as well as the opposite effect that vegetation density and flow velocity have on the turbulent kinetic energy (Nepf, 1999), greatly add to the difficulties of predicting

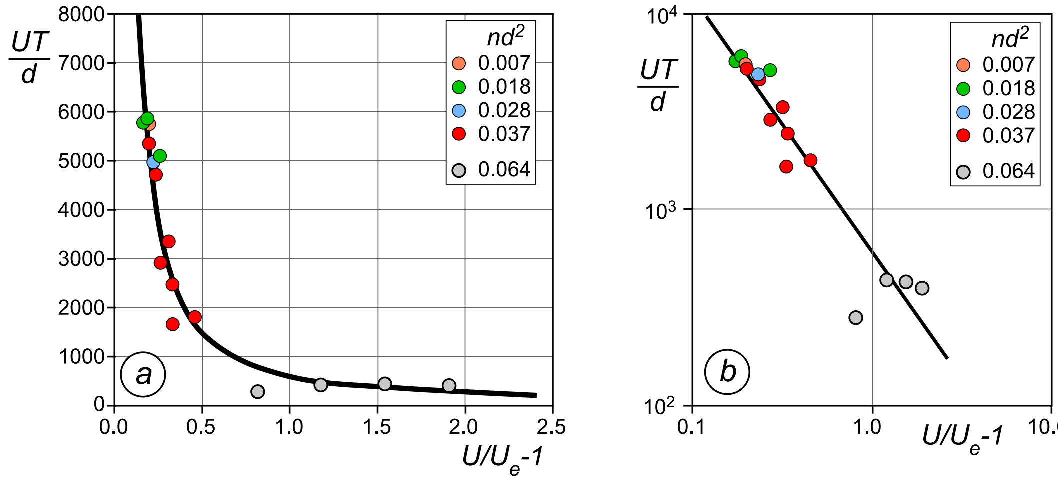

Figure 8. (a) Mean residence time, T, normalized by the ratio d/U, as a function of $U/U_e - 1$. Gray circles denote the values estimated from the experiments performed by Peruzzo et al. (2012); the thick solid line is Equation 13; (b) same as (a) in log-log scale ($R^2 = 0.993$).

seeds dispersal or their definite capture and germination; thereby, the relative importance of the mechanical factors that control the evolution of a vegetation patch needs to be assessed on a case by case basis. From this mechanical point of view, the existence of an optimal vegetation density related to the vegetation type and flow regime cannot be excluded, and the issue deserves to be investigated.

We finally discuss the possibility of estimating the mean velocity of the particle cloud into the array. According to Shi et al. (2021), the mean transport velocity of floating particles, U_m, reads

$$U_m = \frac{U}{1+\omega} \qquad \text{with} \qquad \omega = \frac{P_i P_t}{1 - P_i P_c} \frac{UT}{\Delta s} \tag{14}$$

We use the experimental values for the velocity U and the interaction probability P_i, and the extrapolated values for P_c, P_t and for the mean residence time, T to compute the parameter ω and hence the transport velocity U_m with Equation 14.

This theoretical value for U_m is compared with the experimental one estimated with the following procedure: (a) for each experimental condition we consider all the recorded paths, their length L_i, and the time Δt_i spent by particles to travel the distance L_i ($i = 1, N$; with N the number of paths); (b) we then consider all the temporary capture events lasting $\tau_{ij} < t_{obs}$ ($j = 1, N_j$; with N_j the number of temporary capture events in the ith path); (c) we compute the total time during which the particle was traveling, $T_{run} = \sum_i \Delta t_i - \sum_i \sum_j \tau_{ij}$, and the number of temporary capture events, $N_{tt} = \sum_i L_i/\Delta s P_i P_t$; (d) the mean transport velocity is then computed as $U_m = \sum_i L_i/(T_{run} + N_{tt} T)$.

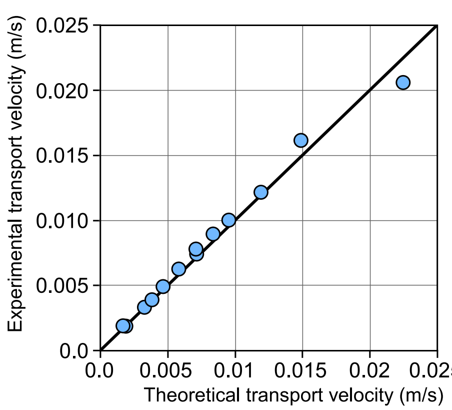

Figure 9. Comparison between the theoretical and experimental mean transport velocity of floating particles, U_m.

The experimental mean transport velocities of floating particles are compared with the theoretical ones in Figure 9; all points are close to the line of perfect agreement ($R^2 = 0.9948$), confirming the reliability of Equation 14.

4. Conclusions

This research sought to extend knowledge about the interaction processes between emergent vegetation and floating particles, such as seeds and propagules, through laboratory experiments. In particular, we focused on the temporary capture process that greatly affects the particle dispersion.

On one hand, we have verified that the overall probability that a particle is captured by a stem, $P_t + P_c$, is rather independent of the stem density n. In other words, the probability $P_c + P_t$ in the present experiments with an array of cylinders corresponds to the probability P_{c0} in the experiments with a single cylinder performed by Peruzzo et al. (2016), in which a negligibly small number of temporary capture events was observed.

On the other hand, we observed that the fraction of captured particles that, for the same velocity U, are temporarily captured, $P_t/(P_c + P_t)$, increases with stem density. This behavior is found to be strictly related to the turbulent kinetic energy produced by the vegetation. We also proposed a simple equation relating $P_t/(P_c + P_t)$ to turbulent kinetic energy k that fits well to the experimental data.

The probability $P_c + P_t$ as well as the relative mean retention time TU/d, in the temporary capture events, are both a function of the relative flow velocity U/U_e, with U_e the escape velocity; when U/U_e is smaller than approximately one, then $P_t + P_c \cong 1$, and the relative retention time approaches infinity.

We found that the escape velocity turns out to be a key parameter controlling the fate of floating seeds and propagules; in fact all model parameters, that is, P_i, $P_t + P_c$, and T, scale with U_e. It should be stressed that this velocity scale is determined by the specific features of both the particle and the stem (body size, particle density, and materials); therefore, it is reasonable to extend the outcomes to seeds and stems of different species, provided that their shapes are not significantly different from those adopted in the present experiments, that is, sphere and circular cylinder, respectively. On the contrary, we could likely observe a substantially different behavior in the retention process with plants having extensive foliage or seeds with large slenderness, as the elongated wetted section causes a spatially variable meniscus elevation (Chambert & James, 2009; Pozrikidis, 2010). Together with U_e, the vegetation density, n, plays a major role in the dynamics of floating particles by affecting the interaction probability and, especially, the temporary capture process, hence mechanical diffusion.

Notation

b	distance between the outermost trajectories of particle collision (m)
c_1	calibration factor (−)
c_2	calibration factor (−)
C_D	bulk drag coefficient (−)
d	cylinder diameter (m)
d_p	particle diameter (m)
k	turbulent kinetic energy per unit mass (m^2 s^{-2})
L	length of test section (m)
n	number of stems per unit area (m^{-2})
N_0	number of segments traversed by particles (−)
N_c	number of capture events with retention time longer than
N_i	number of particle-cylinder interactions (−)
N_t	number of capture events with retention time shorter than
P_c	probability that a particle is permanently captured by a stem
P_{c0}	probability that a particle is permanently captured in the
P_i	probability that a particle interacts with a stem (−)
P_t	probability that a particle is temporarily captured by a stem
T	mean value of all retention times (s)
t_{obs}	defined limited observation time (s)
T_{obs}	mean value of retention times which are shorter than
U	surface velocity (m/s)
U_e	escape velocity (m/s)
U_m	mean transport velocity of floating particles (m/s)
α	shape parameter of gamma distribution (−)
α_k	calibration factor (−)
β	rate parameter of gamma distribution (−)
Δs	mean center-to-center distance between adjacent stems (m)
Γ	gamma distribution (−)
η	collision efficiency of the stem (−)

σ	surface tension (N/m)
τ	retention time (s)
ω	dimensionless parameter (−)

Data Availability Statement

The data used in this study are available at http://researchdata.cab.unipd.it/575/.

Acknowledgments
The authors gratefully acknowledge Heidi M. Nepf for the use of the data collected in the Nepf Environmental Fluid Mechanics Lab. This work was supported by the China Scholarship Council (CSC) (Grant No. 201806040205). Open Access Funding provided by Università degli Studi di Padova within the CRUI-CARE Agreement.

References

Chambert, S., & James, C. (2009). Sorting of seeds by hydrochory. *River Research and Applications*, *25*(1), 48–61. https://doi.org/10.1002/rra.1093

Chang, E. R., Veeneklaas, R. M., Buitenwerf, R., Bakker, J. P., & Bouma, T. J. (2008). To move or not to move: Determinants of seed retention in a tidal marsh. *Functional Ecology*, *22*(4), 720–727. https://doi.org/10.1111/j.1365-2435.2008.01434.x

Chang, K., & Constantinescu, G. (2015). Numerical investigation of flow and turbulence structure through and around a circular array of rigid cylinders. *Journal of Fluid Mechanics*, *776*, 161–199. https://doi.org/10.1017/jfm.2015.321

Defina, A., & Peruzzo, P. (2010). Floating particle trapping and diffusion in vegetated open channel flow. *Water Resources Research*, *46*, W11525. https://doi.org/10.1029/2010WR009353

Defina, A., & Peruzzo, P. (2012). Diffusion of floating particles in flow through emergent vegetation: Further experimental investigation. *Water Resources Research*, *48*, W03501. https://doi.org/10.1029/2011WR011147

Defina, A., & Pradella, I. (2014). Vortex-induced cross-flow seiching in cylinder arrays. *Advances in Water Resources*, *71*, 140–148. https://doi.org/10.1016/j.advwatres.2014.06.002

De Ryck, D. J., Robert, E. M., Schmitz, N., Van der Stocken, T., Di Nitto, D., Dahdouh-Guebas, F., & Koedam, N. (2012). Size does matter, but not only size: Two alternative dispersal strategies for viviparous mangrove propagules. *Aquatic Botany*, *103*, 66–73. https://doi.org/10.1016/j.aquabot.2012.06.005

Espinosa-Gayosso, A., Ghisalberti, M., Ivey, G. N., & Jones, N. L. (2013). Particle capture by a circular cylinder in the vortex-shedding regime. *Journal of Fluid Mechanics*, *733*, 171–188. https://doi.org/10.1017/jfm.2013.407

Espinosa-Gayosso, A., Ghisalberti, M., Ivey, G. N., & Jones, N. L. (2015). Density-ratio effects on the capture of suspended particles in aquatic systems. *Journal of Fluid Mechanics*, *783*, 191–210. https://doi.org/10.1017/jfm.2015.557

Lipoma, M. L., Cuchietti, A., Gorne, L. D., & Díaz, S. M. (2019). Not gone with the wind: Vegetation complexity increases seed retention during windy periods in the argentine semiarid chaco. *Journal of Vegetation Science*, *30*(3), 542–552. https://doi.org/10.1111/jvs.12747

Liu, X., Zeng, Y., & Huai, W. (2018). Modeling of interactions between floating particles and emergent stems in slow open channel flow. *Water Resources Research*, *54*, 7061–7075. https://doi.org/10.1029/2018WR022617

Liu, X., Zeng, Y., Katul, G., Huai, W., & Bai, Y. (2020). Longitudinal dispersal properties of floating seeds within open-channel flows covered by emergent vegetation. *Advances in Water Resources*, *144*, 103705. https://doi.org/10.1016/j.advwatres.2020.103705

Nepf, H. (1999). Drag, turbulence, and diffusion in flow through emergent vegetation. *Water Resources Research*, *35*(2), 479–489. https://doi.org/10.1029/1998WR900069

Nepf, H., Mugnier, C., & Zavistoski, R. (1997). The effects of vegetation on longitudinal dispersion. *Estuarine, Coastal and Shelf Science*, *44*(6), 675–684. https://doi.org/10.1006/ecss.1996.0169

Nilsson, C., Brown, R. L., Jansson, R., & Merritt, D. M. (2010). The role of hydrochory in structuring riparian and wetland vegetation. *Biological Reviews*, *85*(4), 837–858. https://doi.org/10.1111/j.1469-185x.2010.00129.x

Palmer, M. R., Nepf, H. M., Pettersson, T. J., & Ackerman, J. D. (2004). Observations of particle capture on a cylindrical collector: Implications for particle accumulation and removal in aquatic systems. *Limnology & Oceanography*, *49*(1), 76–85. https://doi.org/10.4319/lo.2004.49.1.0076

Peruzzo, P., Defina, A., & Nepf, H. (2012). Capillary trapping of buoyant particles within regions of emergent vegetation. *Water Resources Research*, *48*(7), e2012WR011944. https://doi.org/10.1029/2012wr011944

Peruzzo, P., Defina, A., Nepf, H. M., & Stocker, R. (2013). Capillary interception of floating particles by surface-piercing vegetation. *Physical Review Letters*, *111*(16), 164501. https://doi.org/10.1103/physrevlett.111.164501

Peruzzo, P., Viero, D. P., & Defina, A. (2016). A semi-empirical model to predict the probability of capture of buoyant particles by a cylindrical collector through capillarity. *Advances in Water Resources*, *97*, 168–174. https://doi.org/10.1016/j.advwatres.2016.09.006

Peterson, J. M., & Bell, S. S. (2012). Tidal events and salt-marsh structure influence black mangrove (avicennia germinans) recruitment across an ecotone. *Ecology*, *93*(7), 1648–1658. https://doi.org/10.1890/11-1430.1

Pozrikidis, C. (2010). Computation of three-dimensional hydrostatic menisci. *IMA Journal of Applied Mathematics*, *75*(3), 418–438. https://doi.org/10.1093/imamat/hxp035

Rubenstein, D. I., & Koehl, M. A. (1977). The mechanisms of filter feeding: Some theoretical considerations. *The American Naturalist*, *111*(981), 981–994. https://doi.org/10.1086/283227

Rudi, G., Belaud, G., Troiano, S., Bailly, J.-S., & Vinatier, F. (2021). Vegetation cover at the water surface best explains seed retention in open channels. *Ecohydrology*, *14*(2), e2263. https://doi.org/10.1002/eco.2263

Shi, W., Peruzzo, P., & Defina, A. (2021). An Eulerian model for the transport and diffusion of floating particles within regions of emergent vegetation. *Water Resources Research*, *57*, e2021WR029625. https://doi.org/10.1029/2021WR029625

Shimeta, J., & Jumars, P. A. (1991). Physical mechanisms and rates of particle capture by suspension feeders. *Oceanography and Marine Biology an Annual Review*, *29*, 191–257.

Van der Stocken, T., De Ryck, D. J., Vanschoenwinkel, B., Deboelpaep, E., Bouma, T. J., Dahdouh-Guebas, F., & Koedam, N. (2015). Impact of landscape structure on propagule dispersal in mangrove forests. *Marine Ecology Progress Series*, *524*, 95–106. https://doi.org/10.3354/meps11206

Vella, D., & Mahadevan, L. (2005). The "cheerios effect". *American Journal of Physics*, *73*(9), 817–825. https://doi.org/10.1119/1.1898523

Viero, D. P., Pradella, I., & Defina, A. (2017). Free surface waves induced by vortex shedding in cylinder arrays. *Journal of Hydraulic Research*, *55*(1), 16–26. https://doi.org/10.1080/00221686.2016.1217948

White, B. L., & Nepf, H. M. (2003). Scalar transport in random cylinder arrays at moderate Reynolds number. *Journal of Fluid Mechanics*, *487*, 43–79. https://doi.org/10.1017/s0022112003004579